Molecular Imaging
Volume 16: 1-9

DOI: 10.1177/1536012117734485
journals.sagepub.com/home/mix
SAGE

Whole-Body Biodistribution, Dosimetry, and Metabolite Correction of [^{11}C]Palmitate: A PET Tracer for Imaging of Fatty Acid Metabolism

Nana L. Christensen, MLS[1], Steen Jakobsen, PhD[1], Anna C. Schacht, PhD[1], Ole L. Munk, PhD[1], Aage K. O. Alstrup, DVM, PhD[1], Lars P. Tolbod, PhD[1], Hendrik J. Harms, PhD[1], Søren Nielsen, MD, PhD[2], and Lars C. Gormsen, MD, PhD[1]

Abstract

Introduction: Despite the decades long use of [^{11}C]palmitate positron emission tomography (PET)/computed tomography in basic metabolism studies, only personal communications regarding dosimetry and biodistribution data have been published.

Methods: Dosimetry and biodistribution studies were performed in 2 pigs and 2 healthy volunteers by whole-body [^{11}C]palmitate PET scans. Metabolite studies were performed in 40 participants (healthy and with type 2 diabetes) under basal and hyperinsulinemic conditions. Metabolites were estimated using 2 approaches and subsequently compared: Indirect [^{11}C]CO_2 release and parent [^{11}C]palmitate measured by a solid-phase extraction (SPE) method. Finally, myocardial fatty acid uptake was calculated in a patient cohort using input functions derived from individual metabolite correction compared with population-based metabolite correction.

Results: In humans, mean effective dose was 3.23 (0.02) μSv/MBq, with the liver and myocardium receiving the highest absorbed doses. Metabolite correction using only [^{11}C]CO_2 estimates underestimated the fraction of metabolites in studies lasting more than 20 minutes. Population-based metabolite correction showed excellent correlation with individual metabolite correction in the cardiac PET validation cohort.

Conclusion: First, mean effective dose of [^{11}C]palmitate is 3.23 (0.02) μSv/MBq in humans allowing multiple scans using ~300 MBq [^{11}C]palmitate, and secondly, population-based metabolite correction compares well with individual correction.

Keywords
quantitation in molecular imaging, advances in PET/SPECT probes, cardiac imaging, metabolism, PET/CT

Introduction

Several fatty acid consuming organs such as the heart, liver, and brain are not readily available for catheterization, which have hampered previous studies of fatty acid metabolism in these tissues. Noninvasive positron emission tomography/computed tomography (PET/CT) with fatty acid or fatty acid analogue tracers was therefore introduced in the 1990s and has since been used continually to study fatty acid metabolism in the myocardium, brain, and liver.[1-4] Despite the widespread use of [^{11}C]palmitate in human experimental studies, we are only aware of 2 papers in which estimates of [^{11}C]palmitate dosimetry are referenced and then only by personal communication to the authors.[5,6] Dosimetry estimates for human [^{11}C]palmitate studies must therefore be based on International Commission on Radiological Protection (ICRP) 106, in which a common estimate for all [^{11}C]tracers is listed.[7] The ICRP 106

[1] Department of Nuclear Medicine & PET Centre, Aarhus University Hospital, Aarhus C, Denmark
[2] Department of Endocrinology, Aarhus University Hospital, Aarhus C, Denmark

Submitted: 20/03/2017. Revised: 04/09/2017. Accepted: 04/09/2017.

Corresponding Author:
Lars C. Gormsen, Department of Nuclear Medicine & PET Centre, Aarhus University Hospital, DK 8000 Aarhus C, Denmark.
Email: lars.christian.gormsen@clin.au.dk

estimate assumes that a large proportion of the radiotracer is excreted via the urine and that the bladder thus receives significant radiation. This assumption results in a rather high estimate of radiation burden with an effective dose realistic maximum of 11 μSv/MBq. As a consequence, most human studies are estimated to result in a radiation burden exceeding 1 mSv per injection (~300 MBq), which, based on international guidelines, precludes the use of [^{11}C]palmitate for younger and healthy individuals.[8] However, fatty acids are rapidly taken up by most tissues and distributed in the whole body. Moreover, fatty acids are to some extent taken up by the renal cells[9] but are not excreted in the urine,[10] and the bladder is therefore not exposed to a large radiation dose. The actual radiation burden of the radiotracer is therefore likely to be lower as also indicated by the personal communications to Ter-Pogossian[6] and Dence[5] in which dose estimates are in the 3 to 4 μSv/MBq range.

The great advantage of [^{11}C]palmitate as a metabolic radiotracer is that it is indistinguishable from endogenous palmitate and therefore reflects the rapid and sometimes complex metabolism of fatty acids. Unfortunately, this property is also a major obstacle to obtain accurate estimates of [^{11}C]palmitate kinetics. Once injected, [^{11}C]palmitate undergoes rapid oxidation, storage, or even redistribution as triglycerides (TGs), all within the normal duration of a dynamic PET study. This results in the formation of several different [^{11}C] metabolites, which must be identified and subtracted from blood or plasma activity in order to obtain a correct input function. Properly conducted [^{11}C]palmitate dynamic studies therefore entail frequent blood sampling and laborious measurements of [^{11}C] metabolites, which may be estimated via an solid-phase extraction (SPE) method or through an indirect assessment based on the appearance of [^{11}C]CO_2 in the blood.[11] However, previously published data on fatty acid analog–derived metabolites indicate that the between-subject variation may be rather small.[12] For practical purposes, [^{11}C] metabolite correction based on population averages is therefore an appealing possibility allowing for [^{11}C]palmitate PET studies without concomitant blood sampling and individual metabolite measurements.

The combined aim of these studies was therefore first of all to publish human [^{11}C]palmitate dosimetry and biodistribution data, secondly to compare [^{11}C] metabolite correction using either [^{11}C]CO_2 or the fraction of [^{11}C] in free fatty acids (FFAs), thirdly to publish population-based [^{11}C] metabolite correction data in patients with and without type 2 diabetes (T2D), and finally to compare population-based metabolite correction with individual metabolite correction in a validation cohort undergoing a cardiac PET study.

Materials and Methods

Dosimetry and Biodistribution Study (Study 1)

Pig dosimetry study. The experiments were performed in 2 healthy domestic Danish Landrace and Yorkshire female pigs (weighing 68.5-69.0 kg) in accordance with the Danish Animal Experimentation Act (license number 2014-15-2934-01026) and the European Directive 2010/63/EU for protection of laboratory animals. The pigs were fasted overnight (16 hours) with free access to water prior to PET scanning. Upon completion of the PET scans, both pigs were euthanized under full anesthesia by an intravenous overdose of pentobarbital (100 mg/mL).

The pigs were premedicated with a mixture of 75 mg midazolam and 375 mg s-ketamine intramuscularly. After placement of an ear vein catheter, anesthesia was induced with 80 to 150 mg propofol intravenously. Pigs were intubated and anesthesia was maintained by infusion of 68 to 69 mL per hour of an anesthesia mixture containing 300 mg propofol, 50 mg midazolam, and 250 mg s-ketamine per 50 mL. The pigs were mechanically ventilated with approximately 7 L/min of a mixture of 1 part O_2 and 2.2 parts medical air. Catheters were surgically placed in femoral arteries and veins. Physiological parameters (heart rate, body temperature, and oxygen saturation) were monitored and normal porcine values were maintained. Hydration was maintained with a saline drip. During the PET scans, the pigs were placed on their back with head and body immobilized by surgical tape fastened to the retractable scanner bed.

Human dosimetry study. Two healthy male volunteers (age 53 and 54 years) were recruited for a whole-body [^{11}C]palmitate radiation dosimetry PET study that was performed in accordance with the Declaration of Helsinki and was approved by the Central Denmark Region Committees on Health Research Ethics (1-10-72-66-12). Both participants signed a written informed consent to participate. Upon entry, the participants were screened by obtaining their medical history, physical examination, and standard blood tests.

Radiopharmaceutical preparation. The radiosynthesis of [^{11}C]palmitate was performed according to good manufacturing practice standards as described in detail previously.[13]

Positron emission tomography imaging. [^{11}C]Palmitate scans were performed on a Siemens Biograph 64 PET/CT scanner with a 21.8-cm axial field of view (Siemens, Erlangen, Germany). For attenuation correction and organ localization, a low-dose CT scan without contrast enhancement was obtained immediately prior to the PET scans (acquisition parameters: CareDose 4D, 120 kV, 25 mAs, 5.0-mm thickness). One minute after intravenous injection of 386 $\pm$ 8 MBq [^{11}C]palmitate to the pigs and 216 $\pm$ 18 MBq [^{11}C]palmitate to the human participants, 5 consecutive whole-body PET scans for pigs and from head to midthigh for humans were obtained with frame durations 1, 1.5, 2, 2.5, and 3 minutes per bed position, respectively. Porcine data were reconstructed using a 3-dimensional (3D) iterative algorithm including resolution modeling (TrueX), with a voxel size of 4.1 $\times$ 4.1 $\times$ 5 mm, 3 iterations, 21 subsets, and a 3.0-mm Gaussian postfilter. Human data were reconstructed using a 3D iterative algorithm with a voxel size of 4.1 $\times$ 4.1

× 5 mm, 3 iterations, 21 subsets, and a 3.0-mm Gaussian postfilter.

Image analysis and dosimetry. Volumes of interest (VOIs) were manually drawn in organs with a higher activity concentration, relative to the surrounding tissue background, to obtain mean radioactivity concentration (Bq/mL) in each organ at the different time points. In organs with a high tracer concentration, VOIs were defined on the coronal or axial PET images, whereas VOIs in organs with a lower activity concentration were drawn on the low-dose CT images in either coronal or axial plane. The organs identified as source organs were the liver, spleen, heart wall, muscle, bone marrow, and renal parenchyma. Organ doses and effective dose were calculated using OLINDA/EXM 1.0 software package.[14]

Metabolite Correction Studies (Studies 2 and 3)

Study participants. Metabolite correction data were collected during 2 previously unpublished clinical studies. Study 2 consisted of 22 study participants with T2D (age 62 ± 5, body mass index [BMI]: 31 ± 5) and 11 healthy controls (age 62 ± 6, BMI: 27 ± 4). The study was performed in accordance with the Declaration of Helsinki and was approved by the Central Denmark Region Committees on Health Research Ethics (1-10-72-522-12). All participants signed a written informed consent to participate.

Study 3 consisted of 9 healthy individuals investigated during hyperinsulinemia (age 59 ± 7, BMI: 27 ± 4). This study was also performed in accordance with the Declaration of Helsinki and was approved by the Central Denmark Region Committees on Health Research Ethics (1-10-72-104-14). All participants signed a written informed consent to participate.

Study outline—Blood sampling from the dynamic [^{11}C]palmitate PET studies. Patients from study 2 and study 3 underwent similar 50-minute [^{11}C]palmitate PET scans and had venous blood samples drawn and analyzed for [^{11}C] metabolites at 5 time points (10, 20, 30, 40, and 50 minutes).

[^{11}C]Palmitate metabolites—SPE method. The extraction of [^{11}C]-labeled lipid fractions was performed as described elsewhere,[3] with minor modifications. The modified method was validated by adding a small sample of [^{11}C]palmitate to venous blood, followed by extraction and separation of TG, FFAs, and phospholipids (PLs) using Waters Milford, Massachusetts aminopropyl (NH2) short cartridges. [^{11}C]Palmitate was solely eluted from the cartridge with 2% acetic acid in diethyl ether.

Blood samples were centrifuged at 15 000 rpm (1 minute at 4°C), 0.6 mL of plasma were transferred to clean glass tubes, and 2 mL of Dole reagent (1 N HCl: n-hepane:2-propanol solution, 1:10:40 vol/vol) was added. Tubes were vortexed for 30 seconds before and after the addition of 2 mL water and 2 mL n-heptane and centrifuged at 4000 rpm (4 minutes at 4°C) to achieve phase separation. The top organic phase was removed with a Finnpipette and transferred to a collecting glass tube. The aqueous phase was subjected to another round of extraction with n-heptane. The combined organic phases were passed slowly through an SPE column (Sep-pak NH2) (Waters, Milford, Massachusetts), which had been previously activated with n-heptane, and the eluate was collected and counted. The retained fractions containing TG, FFA, and PL were separated by subsequent cartridge elution with 3 mL of n-heptane:isopropanol (1:2), 3 mL of 2% acetic acid in diethyl ether, and 3 mL of methanol, respectively. Samples and solvents were passed through the SPE column by applying positive pressure and the fractions collected in polypropylene tubes. Radioactivity in each fraction was measured in a well counter for 1 minute. However, extraction of TGs from the organic phase, with SPE-NH2 short cartridges (Waters, Milford, Massachusetts) employing this method, was not found satisfying compared to previous reports.[3] Thus, significant amounts of radioactivity were found in the combined organic phase after passage through the SPE cartridge. The radioactive fraction increased significantly during the scan, resembling metabolic behavior of labeled TGs. In contrast, the fraction eluted with 3 mL n-heptane:isopropanol (1:2), where TGs are expected to elute, only yielded very low amounts of radioactivity. Based on these findings, we suggest that radioactive-labeled TGs in blood need to be quantified by combining the radioactive counts of the 2 fractions as done in this study. Therefore, the [^{11}C] FFA parent fraction was calculated by dividing the amount of radioactivity eluted in the FFA tube by the combined amount of radioactivity measured in all tubes.

Determination of [^{11}C]CO_2 in blood. Radiolabeled CO_2 concentrations in blood are commonly determined by a simple in vitro acidification of a whole blood sample, followed by heat treatment (85°C) combined with ultrasonic bath[15] or purging with an inert gas at room temperature.[11] [^{11}C]CO_2 is released from the acidic sample and the remaining activity is compared to a paired alkaline sample in which all radioactivity is retained including [^{11}C]CO_2 as bicarbonate. In this study, simple magnetic stirring at 900 rpm in a fume hood triggered release of [^{11}C]CO_2. The method was validated with cyclotron produced [^{11}C]CO_2 according to a published protocol.[11]

Two 0.5 mL venous whole blood samples were drawn simultaneously during the scan (10, 20, 30, 40, and 50 minutes after intravenous administration of [^{11}C]palmitate) and placed in tubes containing 1.5 mL of isopropyl alcohol and 0.5 mL of 0.9 M sodium bicarbonate. One sample was capped immediately after the addition of 0.5 mL of 0.1 N sodium hydroxide. The other sample was acidified with 0.5 mL of 6 N hydrochloric acid and magnetically stirred vigorously for 10 minutes at room temperature. The radioactivity in each vial was then measured in a well counter for 1 minute and decay corrected to a common time point.

Comparison of individual metabolite correction with population-based metabolite correction. For this particular subanalysis, PET images from study 3 were obtained using a Siemens Biograph 64 PET/CT with a 21.8-cm axial field of view (Siemens). Patients were placed with the heart in the field of view, and a low-dose CT

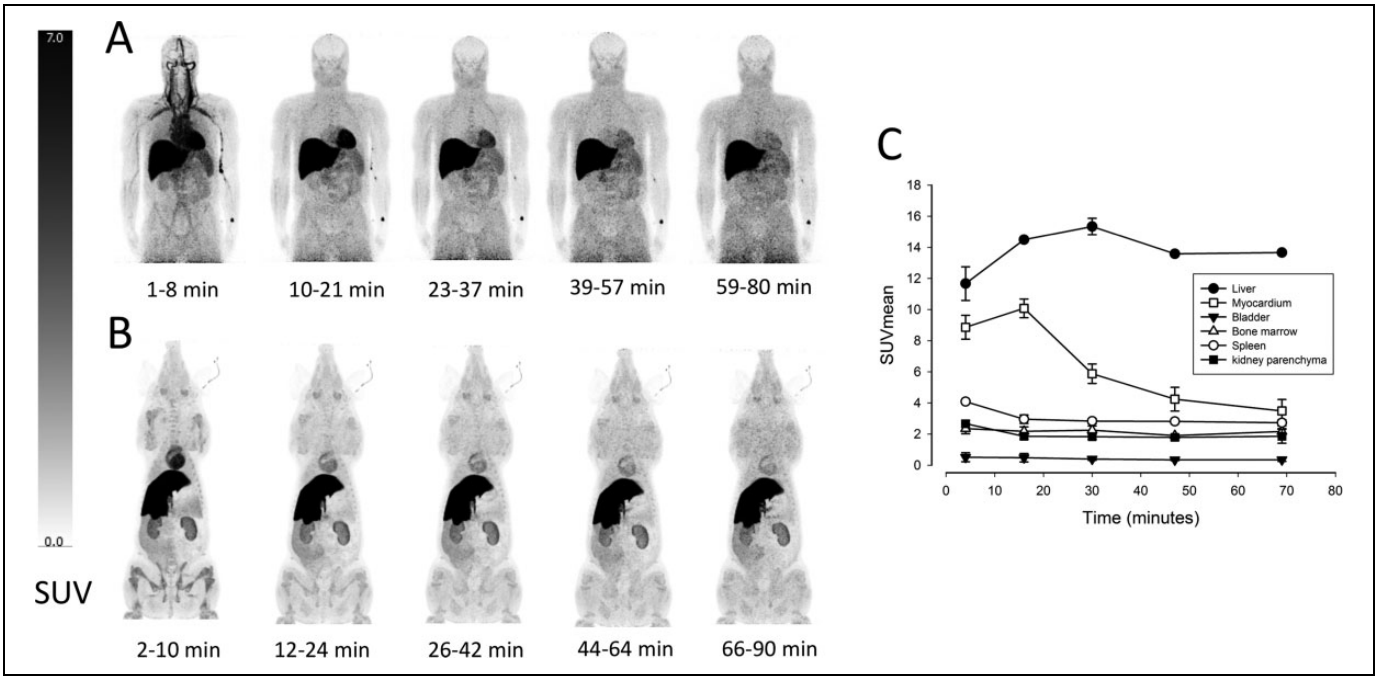

Figure 1. Maximum intensity projections of the biodistribution of [^{11}C]palmitate in 5 successive PET scans in (A) a healthy 54-year old male volunteer and (B) a healthy 4-month-old female pig. Images demonstrate tracer uptake in the liver, heart, kidneys, spleen, bone marrow, and muscles. C, Mean Standardized Uptake Values (SUV) values in organs of interest in the human study. N = 2, mean ± SEM. PET indicates positron emission tomography; SEM, standard error of the mean.

scan was obtained for attenuation and anatomic localization purposes. [^{11}C]Palmitate was injected as a bolus (283 ± 65 MBq) and a 50-minute list mode scan (frame structure 6 × 5 seconds, 6 × 10 seconds, 3 × 20 seconds, 5 × 30 seconds, 5 × 60 seconds, 8 × 150 seconds, 4 × 300 seconds) was performed. Data were reconstructed using a 3D iterative algorithm with a 168 × 168 matrix size, 3 iterations, 21 subsets, and a 5-mm Gaussian postfilter.

The [^{11}C]palmitate corrected for metabolites from study 2 was then used in cardiac image analysis to compare the values of myocardial fatty acid uptake (MFAU) using 2 differently corrected input functions; (1) image-derived input function (IDIF)[16] with hematocrit correction and *individual* [^{11}C] metabolite correction and (2) IDIF with hematocrit correction and *population*-based [^{11}C] metabolite correction. For both approaches, the metabolite-corrected plasma activity curve was calculated by fitting a Hill-function to the metabolite data.

Analysis of MFAU was done by a 3-tissue compartmental model[17] using in-house developed software. The kinetic model and equations are depicted in supplementary Figure 1.

Statistics. Differences in time-activity curves were analyzed by a mixed model repeated measures analysis of variance (ANOVA) where both group and time versus group interactions were considered parameters of interest. Unless otherwise stated, values are given as mean (standard deviation). The Bland-Altman method was used to assess agreement of MFAU calculated using an individual and a population-based metabolite correction factor. A P value <.05 was considered significant. All analyses were performed in SPSS version 21.

Results

Biodistribution and Radiation Dosimetry

The porcine whole-body biodistribution of [^{11}C]palmitate during 5 successive PET scans with a total duration of approximately 90 minutes is illustrated in Figure 1A. The tracer rapidly accumulated in the heart and liver. Furthermore, activity was seen in kidneys, bone marrow, and muscle tissue. There was no measurable urinary excretion of the tracer. The human biodistribution of [^{11}C]palmitate is depicted in Figure 1B. As in the pigs, a high tracer uptake was seen in the heart and liver and with slightly lower concentrations in the kidneys and bone marrow, when compared to the pig scans. Considerably, higher uptake was seen in the spleen and muscle tissue, when compared to the pig scans. As in the pig scans, there was no measurable urinary excretion of the tracer. Absorbed dose estimates and effective doses from both pigs and humans are summarized in Table 1. In the pig study, the absorbed doses were highest in the liver (19.1 μSv/MBq), kidneys (7.4 μSv/MBq), spleen (4.0 μSv/MBq), and heart wall (6.3 μSv/MBq). In the human study, the highest absorbed doses were seen in the liver (27.5 μSv/MBq), heart wall (10.6 μSv/MBq), and spleen (6.3 μSv/MBq). The mean effective doses in the human and pig study were 3.23 μSv/MBq and 2.99 μSv/MBq, respectively.

Metabolite Analysis

[^{11}C] metabolites measured directly by the SPE or indirectly by [^{11}C]CO_2 determination. The fraction of parent [^{11}C]palmitate

Table 1. Radiation Dosimetry of [^{11}C]Palmitate: Absorbed Dose Estimates and Effective Doses in Both Pigs and Humans.

Target Organ	Mean Human Doses (SD), μSv/MBq	Mean Pig Doses (SD), μSv/MBq
Adrenals	3.36 (0.04)	3.18 (0.23)
Brain	0.94 (0.11)	1.41 (0.49)
Breasts	1.35 (0.05)	1.58 (0.28)
Gallbladder wall	4.93 (0.13)	4.25 (0.81)
Lower large intestine wall	1.63 (0.10)	2.05 (0.44)
Small intestine	2.01 (0.08)	2.34 (0.33)
Stomach wall	2.16 (0.04)	2.36 (0.22)
Upper large intestine wall	2.24 (0.06)	2.47 (0.21)
Heart wall	10.57 (1.60)	6.30 (0.43)
Kidneys	5.00 (0.30)	7.42 (1.17)
Liver	27.50 (1.70)	19.05 (9.40)
Lungs	2.14 (0.01)	2.21 (0.11)
Muscle	2.77 (0.04)	2.68 (0.13)
Ovaries	1.81 (0.09)	2.19 (0.40)
Pancreas	3.04 (0.20)	3.09 (0.09)
Red marrow	2.37 (1.20)	2.79 (0.33)
Osteogenic cells	2.12 (1.10)	3.00 (0.62)
Skin	0.99 (0.28)	1.40 (0.27)
Spleen	4.23 (2.88)	3.99 (0.21)
Testes	1.10 (0.30)	1.64 (0.38)
Thymus	1.60 (0.25)	1.97 (0.32)
Thyroid	1.25 (0.29)	1.77 (0.38)
Urinary bladder wall	1.45 (0.30)	2.02 (0.42)
Uterus	1.61 (0.31)	2.18 (0.42)
Total body	2.22 (1.04)	2.92 (0.04)
Effective dose	3.23 (0.02)	2.99 (0.19)

Abbreviation: SD, standard deviation.

present in the FFA pool measured by the SPE method is depicted in Figure 2A. Exact values are given in Table 2. As seen, healthy controls and patients with T2D had largely comparable time-activity curves as evidenced by the nonsignificant difference when analyzed by repeated measures ANOVA ($P = .14$). By contrast, the fraction of radioactivity in the FFA pool was significantly lower in participants during hyperinsulinemia (repeated measures ANOVA $P < .0001$). Figure 2B depicts the fraction of radioactivity present in complex lipids and again, and no difference was observed between healthy controls and patients with T2D ($P = .17$), whereas the fraction was higher in patients during hyperinsulinemia ($P = .02$). Figure 2C depicts the amount of radioactivity detected as [^{11}C]CO_2 by the indirect [^{11}C]CO_2 determination. As expected from the lower amount of parent radioactivity detected in the FFA pool in participants during hyperinsulinemia, release of radioactivity was significantly higher in this group compared with healthy controls and patients with T2D ($P < .01$). Exact values are given in Table 3.

Figure 3 shows combined determination of [^{11}C]palmitate and its more complex metabolites using the SPE method to detect radioactivity in the FFA fraction (left scale) and the indirect [^{11}C]CO_2 determination (right scale). In all 3 patient groups, it is evident that [^{11}C]CO_2 is the predominant metabolite for the first 20 minutes after which [^{11}C] incorporated into

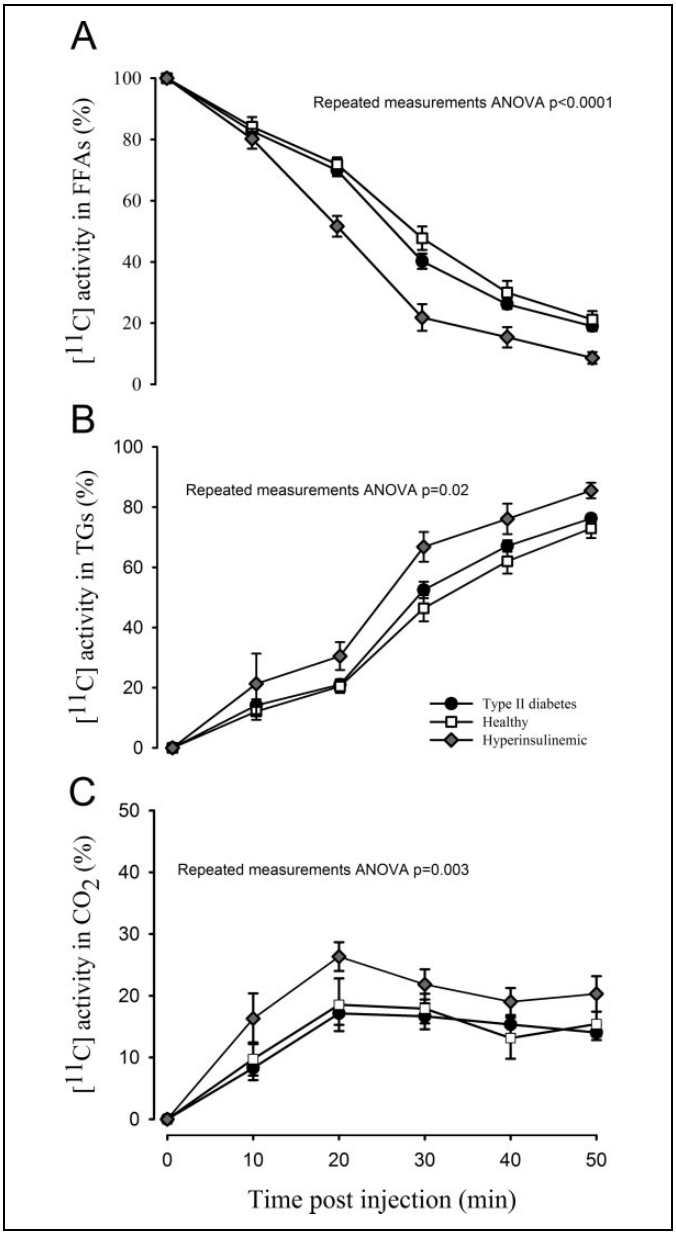

Figure 2. Metabolite correction of palmitate at 5 different time points during a 50-minute dynamic PET scan. A, The amount of radioactivity present as FFAs measured with the SPE method. A repeated measures ANOVA showed significantly lower activity in the FFA fraction in hyperinsulinemic patients (mixed model repeated measures ANOVA [group] $P < .0001$, [group vs time interaction] $P < .0001$). There was no difference in time-activity curves between healthy controls and patients with T2D (mixed model repeated measures ANOVA [group] $P = .14$, [group vs time interaction] $P = .39$). B, [^{11}C] activity in complex lipids (mainly TGs) measured by the SPE method. Significantly more activity was present in this fraction during hyperinsulinemia (ANOVA [group] $P = .02$), whereas no difference was detected between controls and T2D (ANOVA [group] $P = .17$). C, Radioactivity detected in the CO_2 fraction, with significantly more in patients during hyperinsulinemia (ANOVA [group] $P = .003$) and no difference between T2D and controls (ANOVA [group] $P = .72$). Error bars represent $\pm$ standard errors. ANOVA indicates analysis of variance; FFAs, free fatty acids; PET, positron emission tomography; SPE, solid-phase extraction; T2D, type 2 diabetes; TG, triglyceride.

Table 2. The Fraction of Parent [^{11}C]Palmitate Present as FFAs Measured by the SPE Method.

% [^{11}C]Palmitate in the FFA Fraction (SD)			
Time, minutes	Controls	T2D	Hyperinsulinemia
0	100	100	100
10	82.7 (6.5)	84.2 (10.1)	80.2 (8.0)
20	70.0 (8.2)	71.9 (7.1)	51.6 (10.1)
30	40.2 (10.3)	47.8 (12.1)	21.8 (12.4)
40	26.2 (6.2)	30.0 (12.0)	15.4 (10.0)
50	19.0 (6.6)	21.2 (9.2)	8.6 (5.4)

Abbreviations: FFA, free fatty acid; SD, standard deviation; SPE, solid-phase extraction; T2D, type 2 diabetes.

Table 3. Radioactivity Estimated as CO_2 by the Indirect [^{11}C]CO_2 Determination.

% [^{11}C]CO_2 (SD)			
Time, minutes	Controls	T2D	Hyperinsulinemia
0	0	0	0
10	8.3 (7.0)	9.7 (6.6)	16.3 (10.0)
20	17.1 (8.0)	18.5 (10.4)	26.3 (5.7)
30	16.7 (8.9)	17.9 (6.4)	21.8 (6.0)
40	15.3 (6.5)	13.1 (8.9)	19.0 (5.4)
50	14.0 (4.7)	15.4 (5.3)	20.3 (7.0)

Abbreviations: SD, standard deviation; T2D, type 2 diabetes.

complex lipids, overwhelmingly TGs but also to a minor extent (<5%) PLs, increased rapidly (seen as the difference between the 2 curves).

Comparison of kinetic parameters obtained by population-based versus individual metabolite correction. The [^{11}C]metabolite results from 9 healthy controls (from study 3), in which 2 PET scans were performed 3 months apart (n = 18), were used in a cardiac image analysis to compare the values of MFAU. Figure 4 shows the results from the cardiac image analysis using individual and population-based (results obtained from study 2) metabolite correction. The analysis showed an excellent correlation between the individual and population-based metabolite correction methods for measuring MFAU (Pearson correlation coefficient $r = .999$, $P < .001$). Figure 4B depicts the Bland-Altman plot with minimal bias (−0.18; limits of agreement −0.91 to 0.54).

Discussion

In this study, we present biodistribution and radiation dosimetry data of [^{11}C]palmitate in pigs and humans. In addition, we provide population-based metabolite correction data from healthy controls, patients with T2D, and patients during hyperinsulinemia. Finally, estimates of MFAU using individual metabolite correction and population-based metabolite correction were compared.

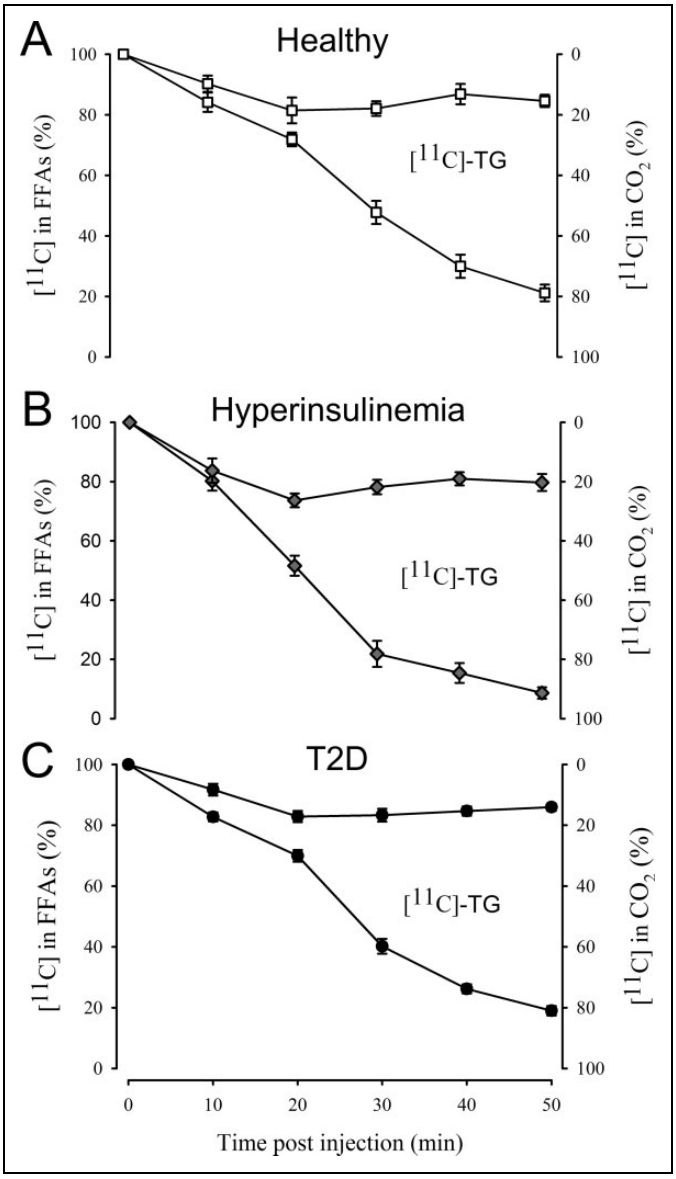

Figure 3. Combined plots showing the individual contributions of the various metabolite fractions to total [^{11}C] activity in healthy controls (A), patients during hyperinsulinemia (B), and patients with T2D (C). The difference between activity in [^{11}C]CO_2 and [^{11}C]palmitate is the area between the 2 curves and represents activity in other fractions (mostly TG). Error bars represent ± standard errors. T2D indicates type 2 diabetes; TG, triglyceride.

[^{11}C]Palmitate Biodistribution and Dosimetry

The radiotracer showed comparable biodistribution and dosimetry data in pigs and humans, indicating that in the absence of human data, dosage values extrapolated from pigs can be used comparatively well. During the 5 successive PET scans, uptake of [^{11}C]palmitate was highest in the liver and heart in both pigs and humans. Dose estimates indicate that the critical organ is the liver, which received an absorbed dose of 19.1 μSv/MBq in pigs and 27.5 μSv/MBq in humans. As expected, there was no measurable urinary excretion of the tracer in neither pigs nor

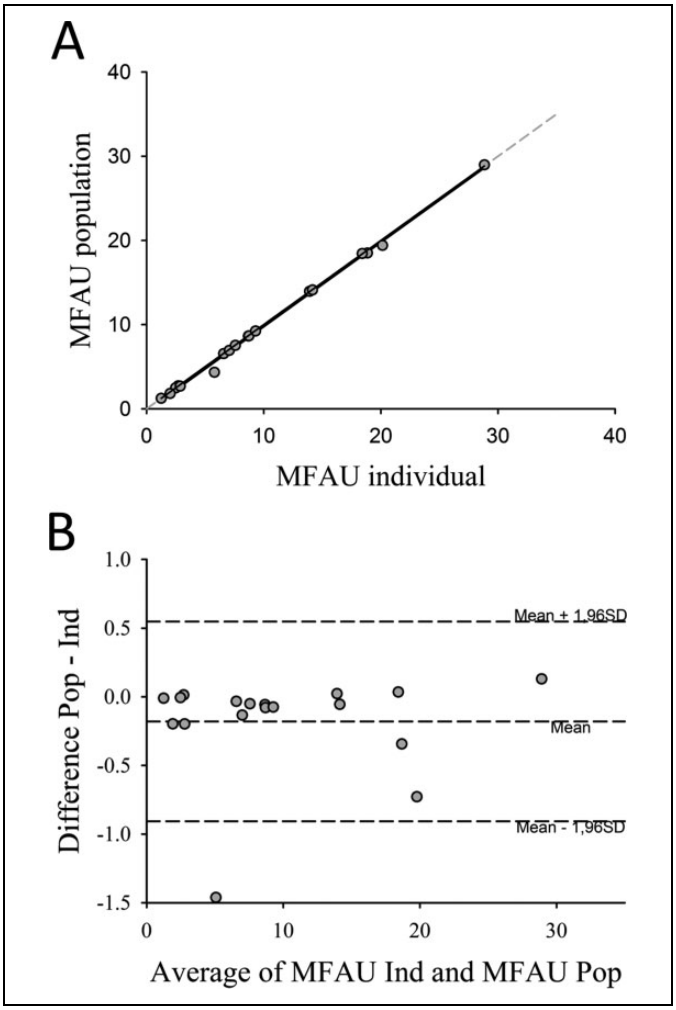

Figure 4. Results from the cardiac image analysis in 9 healthy controls (from study 3), in which 2 PET scans were performed 3 months apart. A, Correlation between individual (ind) and population-based (pop) (results obtained from study 2) metabolite correction methods for measuring MFAU (n = 18). Pearson correlation coefficient $r = .999$, $P < .001$. Regression line equation: $y = -0.200 + 1.002x$. B, Bland-Altman plot. The middle dashed line represents the average difference between the 2 methods; the upper and lower dashed lines represent limits of agreement (mean [1.96 SD]). MFAU indicates myocardial fatty acid uptake; PET, positron emission tomography; SD, standard deviation.

humans, resulting in a rather low radiation burden of the urinary bladder. This observation is hardly surprising since only FFAs not bound to albumin are excreted via glomerular filtration.[10] Only an estimated 0.01% of circulating FFAs are therefore filtrated resulting in very low urinary excretion. We observed few differences in biodistribution between the pigs and humans; compared to the human scans, the pigs showed a higher tracer uptake in kidneys and bone marrow. Furthermore, we saw considerably lower uptake in muscle tissue in pigs, indicating a lower fatty acid metabolism in muscles. This could be explained by the fact that the pigs were anesthetized during the scan procedure[18] and the humans were not.

Using the dosimetry estimates from this study, a typical administration of 300 MBq [^{11}C]palmitate results in a radiation burden of 1.0 mSv, which is within the 1 to 10 mSv range, ICRP find acceptable for volunteers in biomedical research.[8] The low effective dose of [^{11}C]palmitate (3.2 μSv/MBq in humans) is slightly lower than the effective dose estimates observed in other studies using [^{11}C] labeled PET tracers (mean 5.9 μSv/MBq) and allows multiple scans on single participant or use of the tracer as a part of studies with multiple tracers in both healthy and younger individuals.[19]

Metabolite Correction

Circulating FFAs, including [^{11}C]palmitate injected as a bolus, are rapidly taken up by the liver, where they are re-esterified or either oxidized, transformed to ketone bodies, stored in lipid droplets or secreted as very low-density lipoprotein particles.[20] Alternatively, FFAs may be taken up and oxidized by skeletal muscle.[20] In line with this, we detected [^{11}C] activity in the CO_2 fraction 10 minutes after injection, which peaked after 20 minutes and then gradually tapered off as previously reported in miniature pigs and validated in humans.[11] Also in line with previous results, fractional [^{11}C] radioactivity in the TG fraction increased steadily from 10 minutes onward reaching 70% to 80% after 50 minutes.[3] Both [^{11}C]CO_2 and [^{11}C]TG metabolites present in the blood shortly after a bolus injection of [^{11}C]palmitate indicate that correcting only for [^{11}C]CO_2 metabolites may overestimate the amount of unchanged [^{11}C]palmitate. However, as shown in Figure 3, [11C]CO_2 is a pretty robust estimate of total [11C] metabolites in healthy controls and patients with T2D studied under basal postabsorptive conditions. This may not be the case during hyperinsulinemia, as insulin stimulates peripheral tissue fatty acid uptake via the fatty acid transporter protein 1[21] and inhibits adipose tissue hormone sensitive lipase[22] resulting in an accelerated clearance of circulating FFAs. This was evident during this study, where the fraction of unchanged [11C]palmitate decreased rapidly in the patient cohort studied during a hyperinsulinemic-euglycemic clamp. Conversely, the fraction of [^{11}C] activity in TGs was greater during hyperinsulinemia than under basal conditions, which reflects a discretely elevated *relative* appearance of [^{11}C] label in a rapidly decreasing pool of TGs rather than increased *absolute* secretion of [^{11}C]TG from the liver. Our results therefore underscore that metabolite correction using only [^{11}C]CO_2 is not advisable in PET studies performed during hyperinsulinemia.

In contrast, the [^{11}C]palmitate fraction was not significantly different between patients with T2D and healthy age-matched controls, which essentially reflects that fractional catabolic rate of the FFA pool is the same in the 2 groups. The increased fatty acid rate of appearance observed in patients with T2D[23] is offset by the larger FFA pool size[24] resulting in similar clearance of [^{11}C]palmitate. As a practical consequence of this, population-based estimates of [^{11}C]palmitate can be used interchangeably between healthy controls and patients with T2D.

This has also been demonstrated for metabolites of the fatty acid analogue [^{18}F] fluoro-6-thia-heptadecanoic acid.[25]

Population-Based Versus Individual Metabolite Correction

We finally tested whether estimates of myocardial fatty acid kinetics obtained using an input function corrected individually for metabolites differed from estimates obtained using a population-based metabolite correction. This was not the case. There was an excellent correlation between MFAU values obtained by either method, which was also confirmed by the Bland-Altman analysis.

Conclusion

First, the mean effective dose of [^{11}C]palmitate in porcine and human studies was $\sim$3.0 μSv/MBq. This results in a total radiation dose reaching as little as $\sim$1 mSv per human scan, allowing for multiple studies of fatty acid metabolism using $\sim$300 MBq [^{11}C]palmitate. Second, [^{11}C]CO_2 is the predominant metabolite for the first 20 minutes, after which [^{11}C] in complex lipids (TGs and PLs) must be taken into account. Finally, population-based metabolite correction performed well compared with individual metabolite correction in patients with T2D and healthy controls. This allows for simpler study setups in which individual metabolite measurements may be omitted.

Declaration of Conflicting Interests

The author(s) declared no potential conflicts of interest with respect to the research, authorship, and/or publication of this article.

Funding

The author(s) disclosed receipt of the following financial support for the research, authorship, and/or publication of this article: LCG was supported by grants from The Independent Research Fund Denmark and Danish Research Council for Independent Research–Medical Sciences (11-116524/FSS), The Augustinus Foundation, and The Aase and Ejnar Danielsen Foundation.

Supplemental Material

Supplementary material for this article is available online.

References

1. Tamaki N, Fujibayashi Y, Magata Y, Yonekura Y, Konishi J. Radionuclide assessment of myocardial fatty acid metabolism by PET and SPECT. *J Nucl Cardiol*. 1995;2(3):256–266.
2. Karmi A, Iozzo P, Viljanen A, et al. Increased brain fatty acid uptake in metabolic syndrome. *Diabetes*. 2010;59(9):2171–2177. doi:10.2337/db09-0138.
3. Guiducci L, Jarvisalo M, Kiss J, et al. [11C]palmitate kinetics across the splanchnic bed in arterial, portal and hepatic venous plasma during fasting and euglycemic hyperinsulinemia. *Nucl Med Biol*. 2006;33(4):521–528. Research Support, Non-U.S. Gov't 2006/05/25. doi:10.1016/j.nucmedbio.2006.02.003.
4. Kisrieva-Ware Z, Coggan AR, Sharp TL, Dence CS, Gropler RJ, Herrero P. Assessment of myocardial triglyceride oxidation with PET and 11C-palmitate. *J Nucl Cardiol*. 2009;16(3):411–421. doi:10.1007/s12350-009-9051-7.
5. Dence CS, Herrero P, Schwarz SW, Mach RH, Gropler RJ, Welch MJ. Imaging myocardium enzymatic pathways with carbon-11 radiotracers. *Methods Enzymol*. 2004;385:286–315. doi:10.1016/S0076-6879(04)85016-X.
6. Ter-Pogossian MM, Klein MS, Markham J, Roberts R, Sobel BE. Regional assessment of myocardial metabolic integrity in vivo by positron-emission tomography with 11C-labeled palmitate. *Circulation*. 1980;61(2):242–255.
7. . International Commission on Radiological Protection. Radiation dose to patients from radiopharmaceuticals. Addendum 3 to ICRP Publication 53. ICRP Publication 106. Approved by the Commission in October 2007. *Ann ICRP*. 2008;38(1-2):1–197. doi:10.1016/j.icrp.2008.08.003.
8. Radiological Protection in Biomedical Research. A report of Committee 3 adopted by the International Commission on Radiological Protection. *Ann ICRP*. 1991;22(3):1–28, v-xxiv.
9. Druilhet RE, Overturf ML, Kirkendall WM. Structure of neutral glycerides and phosphoglycerides of human kidney. *Int J Biochem*. 1975;6:893–901.
10. Hagenfeldt L. Renal excretion of free fatty acids. *Clin Chim Acta*. 1971;32(3):471–474.
11. Ng Y, Moberly SP, Mather KJ, Brown-Proctor C, Hutchins GD, Green MA. Equivalence of arterial and venous blood for [11C]CO2-metabolite analysis following intravenous administration of 1-[11C]acetate and 1-[11C]palmitate. *Nucl Med Biol*. 2013;40(3):361–365. doi:10.1016/j.nucmedbio.2012.11.011.
12. Taylor M, Wallhaus TR, DeGrado TR, et al. An evaluation of myocardial fatty acid and glucose uptake using PET with [18F]fluoro-6-thia-heptadecanoic acid and [18F]FDG in patients with congestive heart failure. *J Nucl Med*. 2001;42(1):55–62.
13. Mock BH, Brown-Proctor C, Green MA, Steele B, Glick-Wilson BE, Zheng QH. An automated SPE-based high-yield synthesis of [11C]acetate and [11C]palmitate: no liquid-liquid extraction, solvent evaporation or distillation required. *Nucl Med Biol*. 2011;38(8):1135–1142. doi:10.1016/j.nucmedbio.2011.05.007.
14. Stabin MG, Sparks RB, Crowe E. OLINDA/EXM: the second-generation personal computer software for internal dose assessment in nuclear medicine. *J Nucl Med*. 2005;46(6):1023–1027.
15. Fox KA, Abendschein DR, Ambos HD, Sobel BE, Bergmann SR. Efflux of metabolized and nonmetabolized fatty acid from canine myocardium. Implications for quantifying myocardial metabolism tomographically. *Circ Res*. 1985;57(2):232–243.
16. Harms HJ, Knaapen P, de Haan S, Halbmeijer R, Lammertsma AA, Lubberink M. Automatic generation of absolute myocardial blood flow images using [15O]H2O and a clinical PET/CT scanner. *Eur J Nucl Med Mol Imaging*. 2011;38(5):930–939. doi:10.1007/s00259-011-1730-3.
17. Bergmann SR, Weinheimer CJ, Markham J, Herrero P. Quantitation of myocardial fatty acid metabolism using PET. *J Nucl Med*. 1996;37(10):1723–1730.
18. Clarke RSJ, Johnston H, Sheridan B. The influence of anaesthesia and surgery on plasma cortisol, insulin and free fatty acids. *Br J Anaesth*. 1970;42(4):295–299.

19. van der Aart J, Hallett WA, Rabiner EA, Passchier J, Comley RA. Radiation dose estimates for carbon-11-labelled PET tracers. *Nucl Med Biol*. 2012;39(2):305–314. doi:10.1016/j.nucmedbio.2011.08.005.
20. Magkos F, Mittendorfer B. Stable isotope-labeled tracers for the investigation of fatty acid and triglyceride metabolism in humans in vivo. *Clin Lipidol*. 2009;4(2):215–230. doi:10.2217/clp.09.9.
21. Wu Q, Ortegon AM, Tsang B, Doege H, Feingold KR, Stahl A. FATP1 is an insulin-sensitive fatty acid transporter involved in diet-induced obesity. *Mol Cell Biol*. 2006;26(9):3455–3467. doi:10.1128/MCB.26.9.3455-3467.2006.
22. Anthonsen MW, Rönnstrand L, Wernstedt C, Degerman E, Holm C. Identification of novel phosphorylation sites in hormone-sensitive lipase that are phosphorylated in response to isoproterenol and govern activation properties in vitro. *J Biol Chem*. 1998;273(1):215–221.
23. Miles JM, Wooldridge D, Grellner WJ, et al. Nocturnal and postprandial free fatty acid kinetics in normal and type 2 diabetic subjects: effects of insulin sensitization therapy. *Diabetes*. 2003;52(3):675–681.
24. Reaven GM, Hollenbeck C, Jeng C, Wu MS, Chen YD. Measurement of plasma glucose, free fatty acid, lactate, and insulin for 24 h in patients with NIDDM. *Diabetes*. 1988;37(8):1020–1024.
25. Turpeinen AK, Takala TO, Nuutila P, et al. Impaired free fatty acid uptake in skeletal muscle but not in myocardium in patients with impaired glucose tolerance: studies with PET and 14(R, S)-[18F]fluoro-6-thia-heptadecanoic acid. *Diabetes*. 1999;48(6):1245–1250.